Inorg. Chem. **XXXX**, *XX*,

Inorganic Chemistry
Article

Polynuclear Lanthanide Hydroxo Complexes: New Chemical Precursors for Coordination Polymers

N. Mahé,[†] O. Guillou,*[,†] C. Daiguebonne,[†] Y. Gérault,[†] A. Caneschi,[‡] C. Sangregorio,[‡] J. Y. Chane-Ching,[§] P. E. Car,[†] and T. Roisnel[||]

Laboratoire de Chimie du Solide et Inorganique Moléculaire, UMR 6511−CNRS−INSA de Rennes, 20 avenue des Buttes de Coësmes, CS 14315, 35043 Rennes Cedex, France, Department of Chemistry, University of Florence, Via della Lastruccia 5, I-50019 Sesto Fiorentino, Italy, Rhôdia Electronics and Catalysis, Centre de Recherches d'Aubervilliers, 52 rue de la Haie Coq, 93308 Aubervilliers, France, and Laboratoire de Chimie du Solide et Inorganique Moléculaire, UMR 6511−CNRS−Université de Rennes 1, 263 avenue du Général Leclerc, CS 74205, 35042 Rennes Cedex, France

Received September 8, 2004

The synthesis of hexanuclear lanthanide hydroxo complexes by controlled hydrolysis led to polymorphic compounds. The hexanuclear entities crystallize in four different ways that depend on the extent of their hydration. The four structures can be described as hexanuclear lanthanide entities with formula $[Ln_6(\mu_6\text{-}O)(\mu_3\text{-}OH)_8(NO_3)_6(H_2O)_{12}]^{2+}$. Two additional NO_3^- ions intercalate between the hexanuclear entities in order to ensure the electroneutrality of the crystal structure. Some crystallization water molecules fill the intermolecular space. The three first families of compounds (**1**–**3**) exhibit crystal structures that have previously been reported. The fourth family of compounds (**4**) is described here for the first time. Its chemical formula is $[Ln_6(\mu_6\text{-}O)(\mu_3\text{-}OH)_8(NO_3)_6(H_2O)_{12}](NO_3)_2\cdot 2H_2O$ (Ln = Gd, Er, and Y). In this paper, the chemical and thermal stabilities of the hexanuclear lanthanide compounds are reported together with the magnetic properties of the Gd(III)-containing species. To use these entities as precursors for new materials, the substitution of the nitrato groups by chloride ions has been studied. Two byproduct compounds have so been obtained: The first (compound **5**) is a nitrato/chloride hexanuclear compound of chemical formula $[Er_6(\mu_6\text{-}O)(\mu_3\text{-}OH)_8(NO_3)_6(H_2O)_{12}](NO_3)Cl\cdot 2H_2O$. The second one (compound **6**) is a polymeric compound in which the hexanuclear entities are linked by an unexpected and original N_2O_4 bridge. Its chemical formula is $[Er_6(\mu_6\text{-}O)(\mu_3\text{-}OH)_8(NO_3)_4(H_2O)_{11}(OH)(ONONO_2)]Cl_3\cdot 2H_2O$. Its crystal structure can be described as the juxtaposition of chainlike molecular motifs. To the best of our knowledge, this is the first example of a coordination polymer synthesized from an isolated polylanthanide hydroxo complex.

1. Introduction

The assembly of metal−organic infinite frameworks via coordination of metal ions with a multifunctional organic ligand is a field of increasing interest.[1−4] Work along this line is motivated by the concept that molecular-based coordination polymers have potential technological applications such as optoelectronic devices and microporous materials for shape-and-size-selective separations and catalysis.[5−8] The advantage of these metal−organic open frameworks is to allow a wide choice in various parameters including diverse electronic properties and coordination geometries of

* To whom correpondence should be addressed. E-mail: olivier.guillou@insa-rennes.fr. Tel: 02 23 23 84 38.
[†] UMR 6511−CNRS−INSA de Rennes.
[‡] University of Florence.
[§] Centre de Recherches d'Aubervilliers.
[||] UMR 6511−CNRS−Université de Rennes 1.

(1) Yaghi, O. M.; Li, H.; Groy, T. L. *J. Am. Chem. Soc.* **1996**, *118*, 9096−9101.
(2) Reneike, T. M.; Eddaoudi, M.; O'Keeffe, M.; Yaghi, O. M. *Angew. Chem., Int. Ed.* **1999**, *38*, 2590−2594.
(3) Chen, B.; Eddaoudi, M.; Hyde, S. T.; O'Keeffe, M.; Yaghi, O. M. *Science* **2001**, *291*, 1021−1023.
(4) Guillou, O.; Daiguebonne, C. *Handb. Phys. Chem. Rare Earths* **2004**, *34*, in press.
(5) Kepper, C. J.; Rosseinsky, M. *Chem. Commun.* **1999**, 375−376.
(6) Chui, S. S.-Y.; Lo, S. M.-F.; Charmant, J. P. H.; Orpen, A. G.; Williams, I. D. *Science* **1999**, *283*, 1148−1150.
(7) Tong, M.-L.; Wu, Y.-M.; Ru, J.; Chen, X. M.; Chang, H.-C.; Kitagawa, S. *Inorg. Chem.* **2002**, *41*, 4846−4848.
(8) Zaman, M. B.; Smith, M. D.; Ciurtin, D. M.; Loyal, H.-C. *Inorg. Chem.* **2002**, *41*, 4895−4903.

10.1021/ic0401086 CCC: $30.25

Published on Web 00/00/0000

the metal ions as well as versatile functions and topologies of organic ligands. Recently, some interesting results have been published in which some transition-metal clusters were linked via polycarboxylate organic anions so forming coordination polymers exhibiting unprecedented large cavities and low densities.[9,10] For several years, some of us have been working in the field of the lanthanide-based coordination polymers.[11−17] Lanthanide ions, owing to their very similar chemical and structural properties but very different physical properties, can lead to materials exhibiting tunable properties via the choice of the rare-earth ion. At the same time, an increasing number of lanthanide hydroxo complexes featuring well-defined cluster-type motifs have been reported.[18−23] Most of these polylanthanide hydroxo complexes have been obtained by reacting, via a one-pot synthesis, a lanthanide perchlorate salt with sodium hydroxide in the presence of the bifunctional amino acid.[24−28] These ligands prevent the formation of the highly insoluble polymeric lanthanide hydroxide and allow one to control the hydrolysis of the lanthanide ions. Many such species have been recently reported ranging from dinuclear to pentadecanuclear lanthanide hydroxo entities.[20,21,26,29−32] However, these entities present a high positive charge (for instance, hexalanthanide hydroxo species present a charge 8+) and are very unstable in solution.[33] Actually, once these compounds are dissolved, the hydrolysis goes on and the polymeric lanthanide hydroxide precipitates. As a consequence, only a few polymeric systems have been obtained thanks to this method. So, despite this type of serendipitous result, this synthetic route seems to be inappropriate for the design of new coordination polymers.

A second synthetic route, which leads to some hexalanthanide hydroxo complexes,[34,35] was described in the literature some years ago. This route is free of an organic ligand and the starting lanthanide salt is the nitrate, whereas it is the perchlorate in the previously described synthetic route. This alternative route is thus cheaper and safer and, above all, leads to hexanuclear dicationic species. Also the route is based on a subtle balance between the various experimental parameters and the hydroxo complexes studied here to afford a hydrolysis rate (here defined as the number of OH^- groups per lanthanide ion in a given species) of 1.7 very near to the hydrolysis rates of insoluble and very stable polymeric species such as $Er(OH)_2NO_3$[36−39] (hydrolysis rate: 2), $LnONO_3$[40] (hydrolysis rate: 2), and $Ln(OH)_3$[41] (hydrolysis rate: 3). Unfortunately, the synthetic method described in these papers varies with the type of lanthanide ion, and no general synthetic route was available. We decided to rationalize and develop this second synthetic route and study the use of the obtained product compounds as chemical precursors in the design of new coordination polymers. The first results of this study are reported in this paper.

2. Experimental Section

2.1. Preparation of Compounds. Nitrate and chloride lanthanide salts were synthesized by reaction of the corresponding acid with the lanthanide oxide in an aqueous medium according to well-established procedures.[42]

Compounds 1−4. Single crystals or microcrystalline powders are obtained as described in the following.

To a molar solution of $Ln(NO_3)_3 \cdot 5H_2O$ was carefully added a NaOH solution (0.5 mol L^{-1}). When a persistent precipitate appeared, the addition was stopped. The mixture was then heated at 90 °C for a few hours and filtered, and the filtrate was condensed before being left for slow evaporation. After a few days, single crystals appeared.

(9) Eddaoudi, M.; Kim, J.; Rosi, N.; Vodak, D.; Wachter, J.; O'Keeffe, M.; Yaghi, O. M. *Science* **2002**, *295*, 469−472.
(10) Chae, H. K.; Siberio-Perez, D. Y.; Kim, J.; Go, Y.; Eddaoudi, M.; Matzger, A. J.; O'Keeffe, M.; Yaghi, O. M. *Nature* **2004**, *427*, 523−527.
(11) Reneike, T. M.; Eddaoudi, M.; Fehr, M.; Kelley, D.; Yaghi, O. M. *J. Am. Chem. Soc.* **1999**, *121*, 1651−1657.
(12) Serpaggi, F.; Luxbacher, T.; Cheetham, A. K.; Ferey, G. *J. Solid State Chem.* **1999**, *145*, 580−586.
(13) Vaidhyanathan, R.; Natarajan, S.; Rao, C. N. R. *Inorg. Chem.* **2002**, *41*, 4496−4501.
(14) Pan, L.; Woodlock, E. B.; Wang, X. *Inorg. Chem.* **2000**, *39*, 4174−4178.
(15) Daiguebonne, C.; Gérault, Y.; Guillou, O.; Lecerf, A.; Boubekeur, K.; Kahn, O.; Kahn, M. *J. Alloys Compd.* **1998**, *275−277*, 50−53.
(16) Daiguebonne, C.; Guillou, O.; Boubekeur, K. *Structural Diversity in Lanthanide Complex Chemistry: The Ln^{3+}−TMA^{3-}−H_2O System*; Transworld Research Network: Trivandrum, India, 2000; pp 165−183.
(17) Daiguebonne, C.; Deluzet, A.; Camara, M.; Boubekeur, K.; Audebrand, N.; Gérault, Y.; Baux, C.; Guillou, O. *Cryst. Growth Des.* **2003**, *3*, 1015−1020.
(18) Bünzli, J.-C. G.; Piguet, C. *Chem. Rev.* **2002**, *102*, 1897.
(19) Anwander, R. *Angew. Chem., Int. Ed.* **1998**, *37*, 599.
(20) Wang, R.; Zheng, Z.; Jin, T.; Staples, R. J. *Angew. Chem., Int. Ed.* **1999**, *38*, 1813−1815.
(21) Zheng, Z. *Chem. Commun.* **2001**, 2521−2529.
(22) Xu, G.; Wang, Z. M.; He, Z.; Lu, Z.; Liao, C. S.; Yan, C. H. *Inorg. Chem.* **2002**, *41*, 6802−6807.
(23) Plakatouras, J. C.; Baxter, I.; Hursthouse, M. B.; Malik, K. M. A.; McAleese, J.; Drake, S. R. *J. Chem. Soc., Chem. Commun.* **1994**, 2455−2456.
(24) Ma, B. Q.; Zhang, D. S.; Gao, S.; Jin, T. Z.; Yan, C. H.; Xu, G. X. *Angew. Chem., Int. Ed.* **2000**, *39*, 3644−3646.
(25) Ma, B. Q.; Zhang, D. S.; Gao, S.; Jin, T. Z.; Yan, C. H. *New J. Chem.* **2000**, *24*, 251−252.
(26) Wang, R.; Liu, H.; Carducci, M. D.; Jin, T.; Zheng, C.; Zheng, Z. *Inorg. Chem.* **2001**, *40*, 2743−2750.
(27) Wang, R.; Selby, H. D.; Liu, H.; Carducci, M. D.; Jin, T.; Zheng, Z.; Anthis, J. W.; Staples, R. J. *Inorg. Chem.* **2002**, *41*, 278−286.
(28) Zhang, D. S.; Ma, B. Q.; Jin, T. Z.; Gao, S.; Yan, C. H.; Mak, T. C. W. *New J. Chem.* **2000**, *24*, 61−62.
(29) Zheng, Z. *Chemtracts*: *Inorg. Chem.* **2003**, *16*, 1−12.
(30) Hubert-Pfalzgraf, L. G.; Miele-Pajot, N.; Papiernik, R.; Vaissermann, J. *J. Chem. Soc., Dalton Trans.* **1999**, 4127−4130.
(31) Wang, R.; Song, D.; Wang, S. *Chem. Commun.* **2002**, 368−369.
(32) Lam, A. W. H.; Wong, W. T.; Wen, G.; Zhang, X. X.; Gao, S. *New J. Chem.* **2001**, *25*, 531−533.
(33) Wang, R.; Carducci, M. D.; Zheng, Z. *Inorg. Chem.* **2000**, *39*, 1836−1837.
(34) Zak, Z.; Unfried, P.; Giester, G. *J. Alloys Compd.* **1994**, *205*, 235−242.
(35) Giester, G.; Unfried, P.; Zak, Z. *J. Alloys Compd.* **1997**, *257*, 175−181.
(36) Rossmanith, K.; Unfried, P. *Monatsh. Chem.* **1989**, *120*, 849−862.
(37) Unfried, P.; Rossmanith, K.; Blaha, H. *Monatsh. Chem.* **1991**, *122*, 635−644.
(38) Unfried, P.; Rossmanith, K. *Monatsh. Chem.* **1992**, *123*, 1−8.
(39) Louër, D.; Louër, M. *Eur. J. Solid State Inorg. Chem.* **1989**, *26*, 241−253.
(40) Pelloquin, D.; Louër, D.; Louër, M. *J. Solid State Chem.* **1994**, *112*, 182−188.
(41) Beal, G. W.; Milligan, W. O.; Dillin, D. R.; Williams, R. J.; McCoy, J. J. *Acta Crystallogr., Sect. B: Struct. Crystallogr. Cryst. Chem.* **1976**, *32*, 2227−2229.
(42) Desreux, J. F. In *Lanthanide Probes in Life, Chemical and Earth Sciences*; Choppin, G. R., Bünzli, J.-C. G., Eds.; Elsevier: Amsterdam, The Netherlands, 1989; p 43.

Table 1. Summary of the Compounds $[Ln_6(\mu_6\text{-}O)(\mu_3\text{-}OH)_8(NO_3)_6(H_2O)_{12}](NO_3)_2{\cdot}nH_2O$ Characterized up to Now

			compounds described in this work						
compound	n	Ln^{ref}							
			Gd	Tb	Dy	Ho	Er	Y	Yb
1	6	Sm^{35}	Gd						
2	5	Gd^{34}, Dy^{35}	Gd	Tb	Dy	Ho	Er	Y	
3	4	Y^{34}, Er^{35}, Yb^{34}					Er		
4	2		Gd	Tb	Dy	Ho	Er	Y	

Four different families of compounds have been obtained by this route. Their chemical formula is $[Ln_6(\mu_6\text{-}O)(\mu_3\text{-}OH)_8(NO_3)_6(H_2O)_{12}](NO_3)_2{\cdot}nH_2O$, with n varying between 2 and 6. Three out of the four crystal structures have already been described (with similar or other lanthanide ions) in the literature,[34,35] while the fourth one is new. Table 1 summarizes the hexanuclear compounds described up to date. All of the filtered powders were microcrystalline and have been assumed, on the basis of their X-ray powder diffraction diagrams, to present one of these four crystal structures.

Anal. Calcd (found) for $[Gd_6(\mu_6\text{-}O)(\mu_3\text{-}OH)_8(NO_3)_6(H_2O)_{12}](NO_3)_2{\cdot}6H_2O$ (**1**): Gd, 49.25 (49.2); N, 5.85 (5.9); O, 42.59 (42.5); H, 2.31 (2.4). Anal. Calcd (found) for $[Er_6(\mu_6\text{-}O)(\mu_3\text{-}OH)_8(NO_3)_6(H_2O)_{12}](NO_3)_2{\cdot}5H_2O$ (**2**): Er, 51.25 (51.3); N, 5.73 (5.8); O, 40.86 (40.7); H, 2.16 (2.2). Anal. Calcd (found) for $[Er_6(\mu_6\text{-}O)(\mu_3\text{-}OH)_8(NO_3)_6(H_2O)_{12}](NO_3)_2{\cdot}4H_2O$ (**3**): Er, 51.73 (51.7); N, 5.78 (5.9); O, 40.41 (40.3); H, 2.08 (2.1). Anal. Calcd (found) for $[Er_6(\mu_6\text{-}O)(\mu_3\text{-}OH)_8(NO_3)_6(H_2O)_{12}](NO_3)_2{\cdot}2H_2O$ (**4**): Er, 52.71 (52.8), N, 5.88 (6.0); O, 39.51 (39.4); H, 1.90 (1.8).

All of the compounds present similar IR spectra (cm^{-1}): 3550−3100 (s), 1630 (m), 1488 (m), 1461 (m), 1387 (s), 1340 (s), 1040 (w), 800 (w), 615 (w), 526 (w), 421 (w).

All of these compounds have been obtained with various yields depending on the involved lanthanide ion (yields: 17% Gd, 15% Tb, 17% Dy, 25% Ho, 30% Er, 20% Tm, 15% Yb, and 27% Y). The best yield (30%) is obtained for the synthesis of $[Er_6(\mu_6\text{-}O)(\mu_3\text{-}OH)_8(NO_3)_6(H_2O)_{12}](NO_3)_2{\cdot}4H_2O$. As a consequence, most of the studies described hereafter have been performed using it.

Compound 5. Single crystals were obtained as follows. To an equimolar (0.5 $molL^{-1}$) solution of $Ln(NO_3)_3{\cdot}5H_2O$ and $LnCl_3{\cdot}6H_2O$ was added a NaOH solution (0.5 mol L^{-1}). When a persistent precipitate appeared, the addition was stopped. The mixture was heated at 90 °C and filtered, and the filtrate condensed before having been left for evaporation. After a few days, single crystals appeared.

Anal. Calcd (found) for $[Ln_6(\mu_6\text{-}O)(\mu_3\text{-}OH)_8(NO_3)_6(H_2O)_{12}](NO_3)Cl{\cdot}2H_2O$: Er, 53.46 (53.5); N, 5.22 (5.1); O, 37.50 (37.6); H, 1.93 (2.0); Cl, 1.89 (1.8).

IR (cm^{-1}): 3550−3100 (s), 1630 (m), 1488 (m), 1461 (m), 1387 (s), 1340 (s), 1040 (w), 800 (w), 615 (w), 526 (w), 421 (w).

Compound 6. Single crystals were obtained as follows. To a saturated solution of compound **3** in DMF was added a $LnCl_3{\cdot}6H_2O$ (0.5 mol L^{-1}) solution. The mixture was then heated at 90 °C and condensed at 100 °C under vacuum before having been left for evaporation. After a few days, some single crystals appeared.

Anal. Calcd (found) for $[Ln_6(\mu_6\text{-}O)(\mu_3\text{-}OH)_8(NO_3)_4(H_2O)_{11}(OH)(ONONO_2)]Cl_3{\cdot}2H_2O$: Er, 54.15 (54.2); N, 4.53 (4.5); O, 33.67 (33.7); H, 1.91 (1.9); Cl, 5.74 (5.7).

IR (cm^{-1}): 3550−3100 (s), 1630 (m), 1488 (m), 1461 (m), 1387 (s), 1340 (s), 1040 (w), 800 (w), 615 (w), 526 (w), 421 (w).

2.2. X-ray Structure Determinations. All single crystals were sealed in glass capillaries for X-ray single-crystal data collection. Crystals were mounted on a Nonius Kappa CCD diffractometer at room temperature with Mo Kα radiation (λ = 0.710 73 Å). Preliminary cell constants were determined from reflections obtained on 10 frames (1° φ rotation per frame). For the data collection, a crystal-to-detector distance of 25.0 mm has been used and data collection strategies (determination and optimization of the detector and goniometer positions) were performed with the help of the COLLECT program[43] to measure Bragg reflections of the asymmetric triclinic basal unit cell. The reflections were indexed, Lorentz polarization corrected, and then integrated by the DENZO program of the Nonius Kappa CCD software package.[44] Structure determinations were performed with the solving programs SIR97[45] and SHELXL97,[46] which revealed all of the non-hydrogen atoms. All non-hydrogen atoms of the hexanuclear entity were refined anisotropically using the SHELXL program. The oxygen atoms of the crystallization water molecules and the localized intercalated nitrato groups were refined anisotropically. The disordered intercalated nitrato groups were refined isotropically. Hydrogen atoms of the water molecules were not localized.

Crystal data and structure refinement of the six compounds are available in the Supporting Information. The characterization of the obtained microcrystalline powders has been assumed on the basis of comparisons between experimental powder X-ray diffraction (XRD) diagrams and calculated ones from crystal structures. The calculated XRD diagrams have been performed using POWDERCELL[47] software and compared with the experimental ones using WINPLOTR[48] software.

Full details of the X-ray structure determination of compounds **2**−**6** have been deposited with the Fachinformationszentrum Karlsruhe under the depository numbers CSD-414225, CSD-414323, CSD-414224, CSD-414326, and CSD-414318, respectively, and can be obtained, upon request, from the authors.

2.3. Magnetic Measurements. The temperature dependence of the magnetic susceptibility was measured on polycrystalline powders using a Cryogenic S600 SQUID magnetometer in the temperature range of 2.0−300 K with magnetic fields of 0.1 and 1 T. Diamagnetic corrections of the constituent atoms were estimated from Pascal's constants.[49]

2.4. Thermal Analysis Measurements. Thermogravimetric/differential thermal analyses (TG/DTA) were performed using a Perkin-Elmer Pyris Diamond instrument while flowing N_2 or air (100 mL min^{-1}) with a heating rate of 5 °C min^{-1} between 25 and 1000 °C in a Pt crucible.

2.5. Thermal Dependence X-ray Diffraction (TDXD). TDXD analysis was performed using a Philips diffractometer using Cu $K\alpha_1$ radiation in the range of 5−70° in 2θ. The heating of the sample was effected by an Anton Paar HTK 1200 furnace. During the analysis, the sample was held under a N_2 flux (100 mL min^{-1}).

2.6. Solubility Measurements and Stability Controls. For these studies, commercial solvents have been used without further purification or desiccation. A suspension of 500 mg of a thermally dehydrated Er(III)-based hexanuclear compound in 20 mL of solvent was left under stirring, at room temperature, overnight, in a capped vessel. The mixture was then filtrated, and the Er^{3+} ion concentra-

(43) *COLLECT: Kappa CCD software*; Nonius: Delft, The Netherlands, 1998.
(44) Otwinowski, Z.; Minor, W. *Methods Enzymol.* **1997**, 307−326.
(45) Altomare, A.; Burla, M. C.; Camalli, M.; Cascarano, G.; Giacovazzo, C.; Guagliardi, A.; Moliterni, A. G. G.; Polidori, G.; Spagna, R. *J. Appl. Crystallogr.* **1999**, *32*, 115−119.
(46) Sheldrick, G. M.; Schneider, T. R. *Methods Enzymol.* **1997**, 319−343.
(47) Kraus, W.; Nolze, G. *J. Appl. Crystallogr.* **1996**, *29*, 301−303.
(48) Roisnel, T.; Rodriguez-Carjaval, J. *Mater. Sci. Forum* **2000**, 118−123.
(49) O'Connor, C. J. *Prog. Inorg. Chem.* **1982**, *29*, 203.

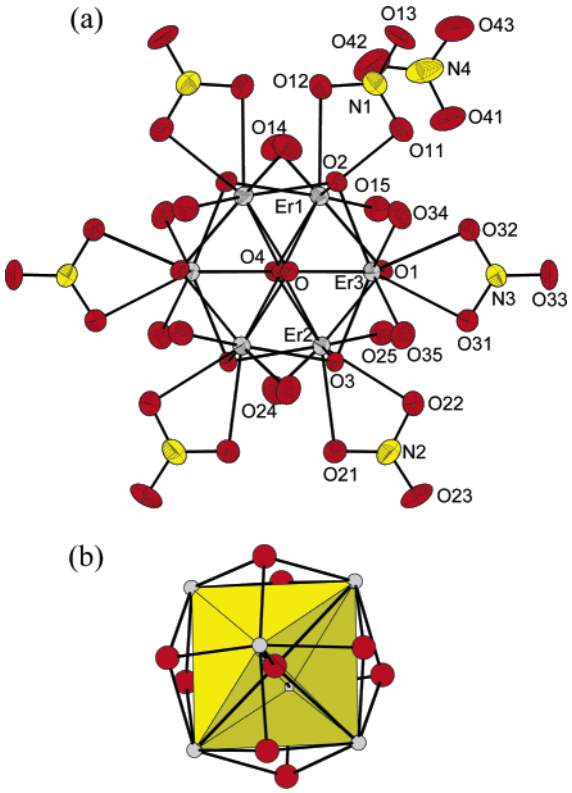

Figure 1. (a) View of the hexanuclear entity $[Er_6(\mu_6\text{-}O)(\mu_3\text{-}OH)_8(NO_3)_6(H_2O)_{12}]^{2+}$ along with the labeling scheme. (b) Simplified view of the hexanuclear entity $[Er_6(\mu_6\text{-}O)(\mu_3\text{-}OH)_8(NO_3)_6(H_2O)_{12}]^{2+}$ emphasizing the quasi-perfect lanthanide ions made octahedron. For clarity, only oxygen atoms (large circles) and lanthanide ions (small circles) have been drawn.

tion in the solution was measured using a JY24 ICP spectrometer. The remaining solid was analyzed by powder XRD.

To check if the hexanuclear entities were destroyed or not in solution, the filtrates were concentrated to dryness and the obtained powder was analyzed by XRD.

3. Result and Discussion

3.1. Description of the Structure of $[Er_6(\mu_6\text{-}O)(\mu_3\text{-}OH)_8(NO_3)_6(H_2O)_{12}](NO_3)_2\cdot 2H_2O$ (Family 4). The crystal structure of this compound consisted of lanthanide-based hexanuclear entities of chemical formula $[Er_6(\mu_6\text{-}O)(\mu_3\text{-}OH)_8(NO_3)_6(H_2O)_{12}]^{2+}$. Two nitrato counterions ensure the neutrality of the crystalline framework, and two crystallization water molecules complete the crystal structure.

The hexanuclear entity can be described as follows. An O^{2-} ion is surrounded by six lanthanide ions in an octahedral fashion. So, one contact between the lanthanide ions is ensured by a μ_6-oxo bridge. The Er−O distances are roughly 2.48 Å, and the shortest Er−Er distances in the octahedron lie in the range of 3.5−5 Å (see Figure 1). Each of the faces of this octahedron is capped by a μ_3-OH group with all Er−O distances around 2.3 Å. This bridge ensures the second contact between the lanthanide ions. To complete the coordination spheres of the lanthanide ions, each of them is bound by a bidentate nitrato group and two coordination water molecules. Actually the lanthanide ions are nine coordinated by one central O(II−), four oxygen atoms from the μ_3-hydroxo groups, two oxygen atoms from a bidentate nitrato group, and two oxygen atoms from coordinated water molecules, therefore forming a distorted tricapped trigonal prism.

The crystal packing of this compound can be described as the juxtaposition of six hexanuclear entities per unit cell. The free nitrato groups and the two crystallization water molecules are localized between the hexanuclear entities, therefore forming a complex pseudo-three-dimensional network based on hydrogen bonds.

In this structure, the nitrato group, which ensures the electroneutrality of the crystalline framework, is disordered. The nitrogen atom is perfectly localized, while the three oxygen atoms are disordered in such a way that two equally probable coplanar NO_3^- groups are centered on the same nitrogen atom and rotated from each other by 60°.

3.2. Comparison of the Crystal Structures of Compounds belonging to Families 1−4. In all compounds belonging to families **1**, **2**, or **3**, the hexanuclear entities $[Ln_6(\mu_6\text{-}O)(\mu_3\text{-}OH)_8(NO_3)_6(H_2O)_{12}]^{2+}$ are essentially the same. These families only differ by their crystallographic packings (see Figure 2) and by the number of water molecules of crystallization, which vary between 2 and 6 depending on the considered crystallographic family.

The metric values of interatomic distances of these hexanuclear complexes are homogeneous and are reported in Table 2. Considering the large intermolecular distances (greater than 10 Å), it is possible to assume, as far as intermolecular interactions can be neglected, that all of the compounds involving the same lanthanide ion exhibit the same physical properties whatever their hydration rate is (this assumption has been checked and confirmed). Identically, all of the compounds exhibit the same chemical and thermal stabilities whatever their initial hydration rate or the involved lanthanide ion are.

3.3. Magnetic Analysis. The variation of the magnetic susceptibility per Gd_6 unit, χ_M, as a function of temperature T was measured between 2 and 300 K. The result is shown in Figure 3 in the form of a $\chi_M T$ versus T plot. At room temperature, $\chi_M T$ is equal to 47.5 $cm^3\ mol^{-1}\ K^{-1}$, which corresponds almost exactly to what is expected for six noninteracting Gd(III) ions. As the temperature is lowered, $\chi_M T$ decreases more and more rapidly, reaching 12.3 $cm^3\ mol^{-1}\ K^{-1}$ at 2 K, indicating that overall weak antiferromagnetic interactions are operating in the compound. The data, plotted as $1/\chi_M$ versus T, were fit to a Curie−Weiss law, giving as best-fit parameters $C = 48.1\ cm^3\ mol^{-1}\ K^{-1}$ and $\theta = -5.3$ K. The field dependence of the magnetization was measured at 2.5 and 4.9 K up to 6 T. In both cases, the magnetization is far from reaching saturation, measuring at the maximum applied fields 35 and 32 μ_B, respectively. Such behavior is again consistent with the presence of weak antiferromagnetic interactions, which because of the large separation between Gd_6 units can be presumably attributed to intracluster exchange interactions.

To evaluate the intensity of the exchange interactions, the measured susceptibility data have been fit using the following model: (i) The hexanuclear entities are supposed to be isolated from each other; that is, the intermolecular interac-

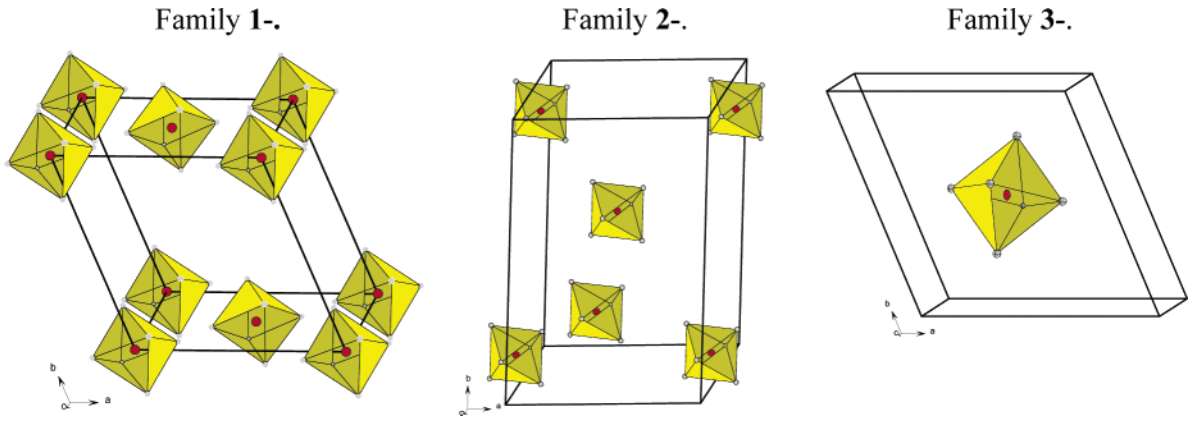

Figure 2. Schematic views of the unit cells of compounds belonging to families **1**−**3**. The octahedrals symbolize the hexanuclear entities.

Table 2. Selected Interatomic Distances (Å) for Compounds Belonging to Families **1**−**4**[a]

	family			
	1 ($n = 6$)	**2** ($n = 5$)	**3** ($n = 4$)	**4** ($n = 2$)
Ln−Ln min−max (μ_3-OH bridge)	3.580−3.649	3.497−3.549	3.473−3.543	3.488−3.535
mean	3.61(4)	3.52(3)	3.51(4)	3.51(3)
Ln−Ln min−max (μ_6-O bridge)	5.078−5.162	4.948−4.989	4.923−5.027	4.931−4.986
mean	5.12(5)	4.97(3)	4.98(6)	4.96(3)
O−O min−max (inter hexanuclear entities)	10.174−11.697	9.953−10.359	10.090−10.130	10.180−11.828
mean	10.9(8)	10.1(2)	10.11(2)	11.0(8)

[a] The general chemical formula is $[Ln_6(\mu_6\text{-}O)(\mu_3\text{-}OH)_8(NO_3)_6(H_2O)_{12}](NO_3)_2 \cdot nH_2O$ with n varying from 6 to 2.

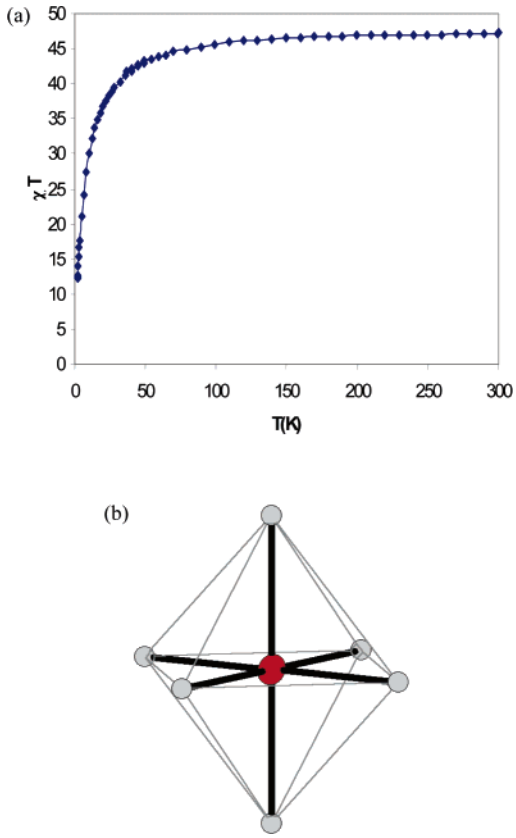

Figure 3. (a) Magnetic measurement for the Gd(III)-containing compound of family **2**. (b) Interacting scheme used for the fitting of the $\chi T = f(T)$ experimental curve.

tions are negligible. (ii) Two different intramolecular Gd−Gd exchange coupling constants have been considered: J_{trans}, describing the Gd−Gd intramolecular interaction through the μ_6-O bridge between trans Gd(III) ions, and J_{cis}, describing the intramolecular interaction via both the μ_6-oxo and μ_3-hydroxo bridges (see Figure 3) connecting cis gadolinium ions. In this model, the exchange interactions within the Gd_6 unit are thus accounted for by the following isotropic spin Hamiltonian:

$$\mathbf{H} = J_{trans}(\mathbf{S}_1\cdot\mathbf{S}_6 + \mathbf{S}_2\cdot\mathbf{S}_4 + \mathbf{S}_3\cdot\mathbf{S}_5) + J_{cis}(\mathbf{S}_1\cdot\mathbf{S}_2 + \mathbf{S}_1\cdot\mathbf{S}_3 + \mathbf{S}_1\cdot\mathbf{S}_4 + \mathbf{S}_1\cdot\mathbf{S}_5 + \mathbf{S}_2\cdot\mathbf{S}_3 + \mathbf{S}_2\cdot\mathbf{S}_5 + \mathbf{S}_2\cdot\mathbf{S}_6 + \mathbf{S}_3\cdot\mathbf{S}_4 + \mathbf{S}_3\cdot\mathbf{S}_6 + \mathbf{S}_4\cdot\mathbf{S}_5 + \mathbf{S}_4\cdot\mathbf{S}_6 + \mathbf{S}_5\cdot\mathbf{S}_6) \quad (1)$$

where $\mathbf{S}_i$ represents the spin operators of the Gd(III) ions and the numbering follows the scheme depicted above.

Susceptibility data were fit by minimizing the sum of the squares of the deviation of the computed χT values from the experimental ones. Theoretical susceptibilities were calculated by full diagonalization of the spin Hamiltonian (1) applying a Boltzmann distribution to populate the spin states. The g value was kept constant and equal to 2.00.

The best-fit parameter values were $J_{trans} = 0.14(8)$ cm^{-1} and $J_{cis} = 0.14(1)$ cm^{-1} with the agreement factor

$$R = \frac{\sum_i |\chi_{obsd}(i)\,T_i - \chi_{calcd}(i)\,T_i|}{\sum \chi_{calcd}(i)\,T_i} = 0.00059$$

The agreement with the experimental data is excellent, notwithstanding the approximations introduced in the calculation. The best-fit curve is compared to the experimental one in Figure 3. As expected, the magnetic exchange interactions between the Gd(III) centers are both weak and of antiferromagnetic nature, yielding a singlet ground spin state. It is also worthwhile to notice that these hexanuclear entities exhibit such antiferromagnetic interaction above 50

Table 3. TG/DTA

temp range (°C)	loss of mass (%): obsd (calcd)	leaving groups	phase (No. JCPDS)
25−100	9.2 (9.3)	$10H_2O$	$[Er_6O(OH)_8(NO_3)_6(H_2O)_6](NO_3)_2$ (unknown)
100−170	14.7 (14.8)	$6H_2O$	$[Er_6O(OH)_8(NO_3)_6](NO_3)_2$ (unknown)
300−360	24.3 (24.1)	$4H_2O$ and $1N_2O_5$	$ErONO_3$ (82-1072)
400−500	40.8 (40.8)	$2N_2O_5$ and $1N_2O_5$	Er_2O_3 (77-0463)

K, while Gd_2O_3 exhibits a perfect Curie behavior between 300 and 2 K.[50] It should also be noted that the two exchange coupling constants are identical. However, as was indeed expected on the basis of the fitting model adopted, large out-of-diagonal elements were observed in the variance/covariance matrix; that is, a number of different couples of parameters were found to satisfactorily reproduce experimental data. This, of course, makes meaningless any discussion about the similarity. Nevertheless, because in all cases small antiferromagnetic exchange coupling constants were obtained, the large observed parameter correlation does not significantly affect the main conclusion about the presence of a weak but sizable intracluster antiferromagnetic interaction.

To confirm that intermolecular interactions are negligible, we measured the magnetic properties of the Gd(III)-containing compound **1**. The results are exactly the same. These values clearly show that the six lanthanide ions are magnetically interacting and that the hexalanthanide hydroxo complex is not simply a topological arrangement of independent ions.

The temperature dependence of the $\chi_M T$ product of the Er analogue measured in the temperature range of 2−300 K. At room temperature, it was 65 $cm^3\ mol^{-1}\ K^{-1}$, close to what was expected for six noninteracting Er^{3+} ions ($11.47 \times 6 = 68.8\ cm^3\ mol^{-1}\ K^{-1}$). Upon decreasing temperature, $\chi_M T$ monotonically decreases, reaching, at 2 K, 27 $cm^3\ mol^{-1}\ K^{-1}$. In this case, the interpretation of the magnetic properties of the cluster is hindered by the large crystal field effect acting on this ion, which alone can justify the observed magnetic behavior, thus masking any eventual weak magnetic intracluster coupling between Er^{3+} ions.

3.4. Thermal Analysis. The thermal behaviors of all of these compounds are essentially the same. Therefore, we only describe here the thermal analysis performed on the Er(III)-containing compound of family **3**. It has been studied by TG/DTA and TDXD under N_2 flux. The TG/DTA (see Table 3) shows that the decomposition occurs in five steps and finally leads (above 500 °C) to Er_2O_3.

The first phenomenon occurs between 25 and 100 °C. It has been attributed to the loss of 10 water molecules per molecular unit [the four crystallization water molecules plus one coordination water molecule per Er(III) ion].

$$[Er_6(\mu_6\text{-}O)(\mu_3\text{-}OH)_8(NO_3)_6(H_2O)_{12}](NO_3)_2\cdot 4H_2O \xrightarrow{25-100\ °C} [Er_6(\mu_6\text{-}O)(\mu_3\text{-}OH)_8(NO_3)_6(H_2O)_6](NO_3)_2 + 10H_2O$$

The six remaining water molecules are lost between 100 and 170 °C, and the resulting phase has been assumed to be the anhydrous hexanuclear compound $[Er_6O(OH)_8(NO_3)_6](NO_3)_2$.

$$[Er_6(\mu_6\text{-}O)(\mu_3\text{-}OH)_8(NO_3)_6(H_2O)_6](NO_3)_2 \xrightarrow{100-170\ °C} [Er_6(\mu_6\text{-}O)(\mu_3\text{-}OH)_8(NO_3)_6](NO_3)_2 + 6H_2O$$

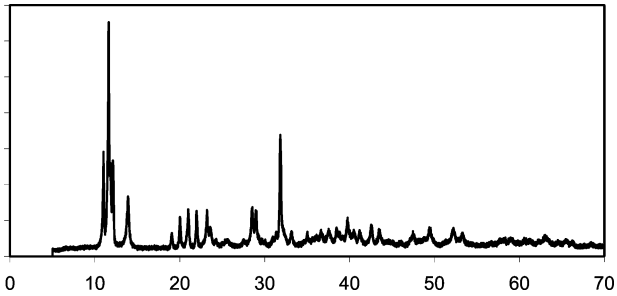

Figure 4. Powder XRD diagram of $[Er_6(\mu_6\text{-}O)(\mu_3\text{-}OH)_8(NO_3)_6](NO_3)_2$. The diagram has been recorded with a Philips diffractometer using the Cu $K\alpha_1$ radiation in the range of 5−70° in 2θ. The observed main picks are listed below. (d (Å):relative intensity) 8.05:41.51; 7.62:100.00; 7.47:37.12; 7.28:38.96; 6.36:22.79; 4.44:13.59; 4.23:17.16; 4.04:15.92; 3.84:14.62; 3.13: 15.25; 3.08:15.25; 2.81:49.91; 2.27:10.24;

This phase is stable over more than 100 °C. Its powder XRD diagram is reported in Figure 4. It can reversibly bind water, reforming the Er(III) compound of family **3**. This phase has been assumed to be the anhydrous hexanuclear entity on the basis of its chemical behavior and elemental analysis. Its structural characterization from its powder XRD diagram has not been successful up to now.

Between 300 and 360 °C, the anhydrous hexanuclear entity decomposes and forms $ErO(NO_3)$ by losing four water molecules and one N_2O_5 molecule per hexanuclear unit.

$$[Er_6(\mu_6\text{-}O)(\mu_3\text{-}OH)_8(NO_3)_6](NO_3)_2 \xrightarrow{300-360\ °C} 6ErO(NO_3) + 4H_2O + N_2O_5$$

The $ErO(NO_3)$ units have been identified from its XRD diagram by using Highscore Software[51] with a JCPDS version PDF2/2000 (sets 1−50 and 70−88) database.

At last, the oxynitrate decomposes in two steps, losing successively two and then one N_2O_5 molecule per six $ErO(NO_3)$ units. This decomposition process has already been described.[52] We finally obtain Er_2O_3, which is characterized from its XRD diagram by using Highscore Software with a JCPDS version PDF2/2000 (sets 1−50 and 70−88) database.

$$6ErO(NO_3) \rightarrow 3Er_2O_3 + 3N_2O_5$$

From this study, it appears that the molecular $[Er_6O(OH)_8(NO_3)_6]^{2+}$ cation is still present at 300 °C. This is rather

(50) Moon, R. M.; Koehler, W. C. *Phys. Rev. B* **1975**, *11*, 1609−1622.
(51) Koninklijke Philips Electronics NV. *X'Pert Highscore*; Philips Analytical BV: Almelo, The Netherlands, 2001.
(52) Haschke, J. M. *Inorg. Chem.* **1974**, *13*, 1812−1818.

interesting as far as industrial applications are considered. To check its thermal stability in air, we have performed a TG/DTA measurement under an air flow. The results of this analysis are exactly the same as those obtained under N_2 flux.

3.5. Solubility and Stability Studies. These compounds are highly soluble in water. Unfortunately, water is not a good medium because a rapid hydrolysis occurs in water and the compounds decompose, leading to the corresponding polymeric hydroxide in few seconds.

To check the ability of these hexanuclear species to be used as chemical precursors, we had to evaluate their solubility and stability in several nonaqueous organic solvents. The results of these tests are as follows: DMSO (21.0 g L^{-1}), DMF (17.5 g L^{-1}), acetone (11.0 g L^{-1}), THF (3.5 g L^{-1}), ethanol (3.5 g L^{-1}), acetonitrile (3.0 g L^{-1}), butan-1-ol (3.0 g L^{-1}), propan-2-ol (2.5 g L^{-1}), diethyl ether (1.5 g L^{-1}), and hexane (0.1 g L^{-1}). Even more, none of the tested solvents destroy the hexanuclear entities.

From this, it appears that, among the tested solvents, DMF is the more convenient one as far as the hexanuclear entities are considered as chemical precursors.

3.6. Synthesis of Chloride-Containing Hexanuclear Entities. To use the hexanuclear entities as precursors for the synthesis of new polymeric compounds, we tried to synthesize hexanuclear entities in which nitrate groups would have been substituted by chloride ions. The availability of such precursors would have afforded some chemical flexibility.

Two synthetic pathways were explored:

The first one consisted of the use of an equimolar mixture of $Ln(NO_3)_3{\cdot}5H_2O$ and $LnCl_3{\cdot}6H_2O$, instead of $Ln(NO_3)_3{\cdot}5H_2O$ only, in the previously described synthesis. The use of the chloride salt only was impossible because its solubility in water was too low. From this synthesis, we did not obtain the expected chloride analogous to the hexanuclear entities but a compound (hereafter named compound **5**) in which a chloride ion substitutes only one of the two intercalated nitrate groups. The hexanuclear entities remain unchanged.

The second route explored consisted of a metathesis in a solvent in which the hexanuclear entities are stable. As already explained, DMF seems to be the best candidate. Once more, we did not obtain the chloride analogous to the hexanuclear entities but surprisingly a polymeric compound hereafter named compound **6**.

3.6.1. Description of the Structure of Compound 5. The crystal structure of this compound consisted of lanthanide hexanuclear entities of formula $[Ln_6(\mu_6\text{-}O)(\mu_3\text{-}OH)_8(NO_3)_6(H_2O)_{12}]^{2+}$ identical with the ones already described. One nitrate group and one chloride ion ensure the neutrality of the crystalline framework. Two water molecules of crystallization are intercalated between the molecular entities.

The crystal packing of this compound can be described by nine hexanuclear entities per unit cell (see Figure 5). The free nitrato group, chloride ion, and crystallization water molecules are localized between the hexanuclear entities, therefore describing a pseudo-three-dimensional network based on a complex hydrogen-bond network.

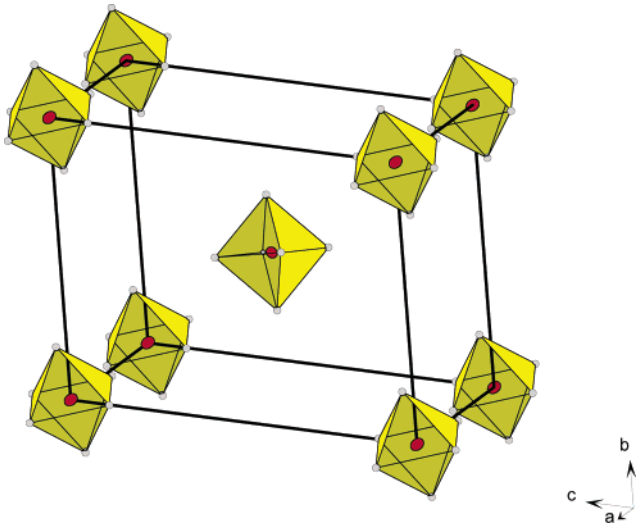

Figure 5. Perspective view of a unit cell of compound **5**. For clarity, only the hexanuclear units have been schematized.

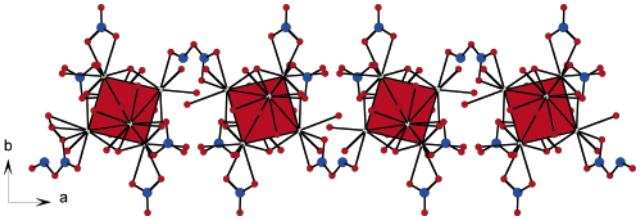

Figure 6. Projection view along the *c* axis of a chainlike molecular motif in compound **6**.

3.6.2. Description of the Structure of Compound 6. This compound has a chemical formula $[Er_6(\mu_6\text{-}O)(\mu_3\text{-}OH)_8(NO_3)_4(H_2O)_{11}(OH)(ONONO_2)]Cl_3{\cdot}2H_2O$ with $a = 16.4039(2)$ Å, $b = 16.1017(2)$ Å, $c = 14.0453(2)$ Å, $\beta = 96.3540(10)°$, and $Z = 4$.

The crystal structure of this compound can be described as the juxtaposition of molecular chainlike motifs spreading along the $a + c$ direction. These chains are constituted by hexalanthanide hydroxo complexes linked to each other via an original N_2O_4 bridge (see Figure 6).

The hexanuclear complexes are very similar to those already described. The central O^{2-} ion is localized on an inversion center ($^1/_2$, $^1/_2$, $^1/_2$). So, three crystallographically independent Er(III) ions are enough for describing the molecular structure. Two out of the three present coordination polyhedra are identical with those previously described; that is, the Er(III) ion is nine coordinated by nine oxygen atoms from two crystallization water molecules, a bidentate nitrate group, four μ_3-hydroxo groups, and the central O^{2-} ion.

On the other hand, the coordination sphere of the third Er(III) atom, namely, Er3, is different. It can be described by two equally probable disordered coordination polyhedra. In one, the Er(III) ion is eight coordinated, whereas in the second one, it is nine coordinated. In both polyhedra, the Er(III) ion is bound to oxygen atoms from four μ_3-hydroxo groups, a coordination water molecule, and the μ_6-oxo central oxygen. The seventh and eighth oxygen atoms that complete the coordination sphere of the eight-coordinated Er3 belong respectively to an additional hydroxo group and to the N_2O_4 bridge, which acts as a unidentate ligand. In the coordination

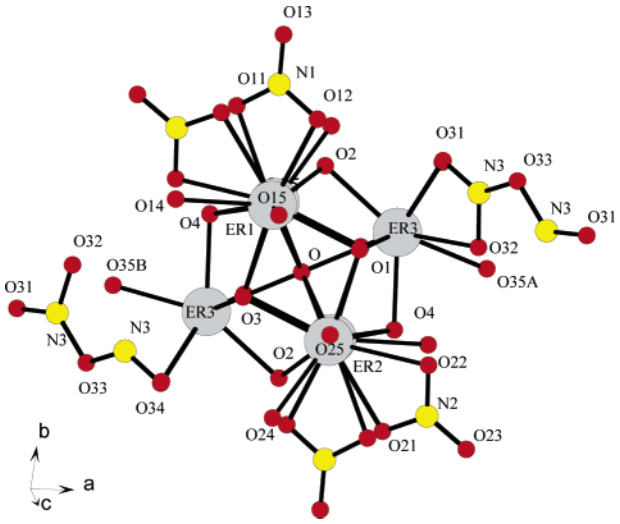

Figure 7. Projection view of a hexanuclear unit in compound **6** along with the labeling scheme.

sphere of the nine-coordinated Er3, the seventh oxygen belongs to an additional coordination water molecule, whereas the eighth and ninth oxygen atoms belong to the N_2O_4 bridge acting as a bidentate ligand (Figure 7). As a consequence of this condensation, the hexanuclear entities present a charge 3+. Indeed, two nitrato anions have condensed in a neutral N_2O_4 molecule, but a hydroxo group has appeared.

The N_2O_4 bridge is very surprising and probably arises from a condensation of two nitrate groups from two adjacent hexanuclear entities. This condensation is certainly favored by the operating mode in which the solution has been evaporated under vacuum at 100 °C. However, this compound is, to the best of our knowledge, the first one exhibiting such a bridge in the field of coordination chemistry. So, we suggest that the formation of this asymmetric nitrite molecule could be catalyzed by the Er(III) ions. This could be linked to the already observed breakdown of the C−C bonds in several lanthanide-containing compounds.[53,54] This asymmetric nitrite molecule has already been observed[55−60] even if no complex of it has been reported so far. The hydroxo group bounded to the disordered Er(III) is necessary for the electroneutrality of the crystal framework. It is also in perfect agreement with the distances Er−O observed in this compound. Indeed, the distance between the oxygen atom from this hydoxo group (O35B) and the Er(III) ion (Er3) is 2.281(13) Å. All of the other Er−OH distances are comprised between 2.2 and 2.4 Å, whereas the Er−OH_2 distances are in the range of 2.4−2.5 Å. The electroneutrality of the crystal framework is ensured by three chloride ions per hexanuclear unit intercalated between the chains. To the best of our knowledge, this last compound is the first polylanthanide hydroxo complex based coordination polymer obtained via a two-step synthesis. So, the existence of this unexpected compound is of great importance for us because it demonstrates the possibility of designing new polylanthanide-based coordination polymers by reacting hexalanthanide hydroxo complexes with organic ligands.

4. Conclusion

We have succeeded in rationalizing the synthesis of hexanuclear hydroxo complexes of the general formula $[Ln_6(\mu_6\text{-}O)(\mu_3\text{-}OH)_8(NO_3)_6(H_2O)_{12}]^{2+}$ (Ln = Gd−Yb). These compounds are thermally rather stable and the molecular entity $[Ln_6(\mu_6\text{-}O)(\mu_3\text{-}OH)_8(NO_3)_6]^{2+}$ does not decompose until 300 °C. They are also suitable for use as chemical precursors in the design of polylanthanide hydroxo complex based coordination polymers. For this purpose, DMF seems to be a very good medium. The availability of these hexalanthanide hydroxo complexes offers a wide range of opportunities. We are currently working on the stabilization of these compounds in various media for different purposes such as medical imaging (in biological media) or catalytic properties (in water or organic media). This stabilization (or increasing of the solubility) could be achieved by the linkage of appropriate organic ligands. The results we have already obtained are very promising but require further work prior to publication. We are also investigating the synthesis of materials in which these hexanuclear species would be linked by organic ligands, therefore forming a porous three-dimensional network. This strategy could lead to materials presenting very high porosity[10] suitable for gas storage for instance.

Acknowledgment. This research was financially supported by the Région Bretagne.

Supporting Information Available: Crystallographic data (in CIF format) and crystal data and structure refinement of compounds **1**−**6**. This material is available free of charge via the Internet at http://pubs.acs.org.

IC0401086

(53) Daiguebonne, C.; Guillou, O.; Baux, C.; Le Dret, F.; Boubekeur, K. *J. Alloys Compd.* **2001**, *323*−*324*, 193−198.
(54) Daiguebonne, C.; Guillou, O.; Kahn, M. L.; Kahn, O.; Oushoorn, R. L.; Boubekeur, K. *Inorg. Chem.* **2001**, *40*, 176−178.
(55) Olson, L. P.; Kuwata, K. T.; Bartberger, M. D.; Houk, K. N. *J. Am. Chem. Soc.* **2002**, *124*, 9469.
(56) Wang, X.; Qin, Q. Z.; Fan, K. J. *THEOCHEM* **1998**, 55.
(57) Wang, J.; Koel, B. E. *Surf. Sci.* **1999**, *436*, 15.
(58) Pinnick, D. A.; Agnew, S. F.; Swanson, B. I. *J. Phys. Chem.* **1992**, *96*, 7092.
(59) Nakamoto, K. *Infrared Spectra of Inorganic and Coordination Compounds*, 2nd ed.; Wiley-Interscience: New York, 1970.
(60) Parts, L.; Miller, J. T., Jr. *J. Chem. Phys.* **1965**, *43*, 136.